Demonstration of full-parallax three-dimensional holographic display on commercial 4 K flat-panel displayer

Frank C. Fan*, Sam Choi, and C. C. Jiang

AFC Technology Co., Ltd., Shenzhen 518104, China

**Corresponding author: drfan@afctech.com*

Received September 1, 2015; accepted November 4, 2015; posted online December 21, 2015

A novel method for a full-parallax three-dimensional (3D) holographic display by means of a lens array and a holographic functional screen is proposed. The process of acquisition, coding, restoration, and display is described in detail. It provides an efficient way to transfer the two-dimensional redundant information for human vision to the identifiable 3D display for human eyes. A holo-video system based on a commercial 4 K flat-panel displayer is demonstrated as the result.

OCIS codes: 090.2870, 100.6890.

doi: 10.3788/COL201614.010007.

Based on the principle of the holographic stereogram, we have published Letters to realize a full-color and real-time holographic display by means of a holographic functional screen (HFS) combined with a system formed by a camera-projector array[1–5]. In practice, it is difficult to integrate the whole system due to the calibration of each individual camera-projector; meanwhile, the high cost of adapting masses of camera-projectors makes such a system unacceptable for public consumption.

Integral photography[6] theoretically seems like an ideal approach for both the acquisition and restoration of three dimensional (3D) light fields; however, it is difficult to overcome the inherent inconsistency formed by the microlens between the sub-image quality and the resolution of the final 3D display because of diffraction effect of the lens aperture. Therefore, a satisfactory 3D display is a challenge that has yet to be overcome.

In this Letter, we propose a novel approach to realize a perfect holographic display perceived by human eyes. It is equivalent to the setup in Refs. [1–5], while the optical axis of each individual camera-projector is parallel to each other, i.e., anchored at an infinitely far point. It could be thought of as a successive technical innovation derived from our proposed physical concepts named the *hoxel* and *spatial spectrum*, which are properly defined by the four-dimensional Fourier transform of the wave function of this nature. The purpose is for the most compact design to carry out the application at the lowest cost.

There are four steps in our innovation:

1. Parallel acquisition of the spatial spectrum.

Figure 1 is the sketched map for the parallel acquisition of the spatial spectrum. L_1 is a plate of lens arrays comprised by $M * N$ small lenses with the same imaging parameters, which are denoted by a_1 for the aperture of each lens, d_1 for the concentric distance, and f_1 for the focal length. The viewing angle of each lens could be expressed as $\tan(\Omega/2) = a_1/2f_1$. As the optical axis of each individual lens is parallel to each other, the spatial spectrum $I_{mn}(j,k)$ ($m = 1$ to M, $n = 1$ to N) of a 3D object O acquired by each lens inside its viewing angle Ω corresponds to what we have described before in Refs. [1–5]. The sampling angle of acquisition could be denoted as $\omega_{mn} = d_1/l_1$, and l_1 is the distance between the lens plate L_1 and the object O. S is a light-sensitive component (such as film, CCD, or CMOS, etc.) placed near the focal plane of L_1 with a distance l_1' to the lens plate to record the spatial spectrum $I_{mn}(j,k)$. $J * K$ is the resolution of the digital light-sensitive component corresponding to each imaging unit of the lens plate: $j = 1$ corresponds to J, and $k = 1$ corresponds to K. The corresponding hoxel is denoted as H_{jk}, i.e., the acquired object O is constructed by $J * K$ hoxels, $H_{jk}(m,n)$. The distance between object O and the reference surface P_R is l_3, and the reference point R is located at the center of P_R. Field aperture M_1 is placed between S and L_1 to prevent the crosstalk of each I_{mn}. Compared with the traditional integral

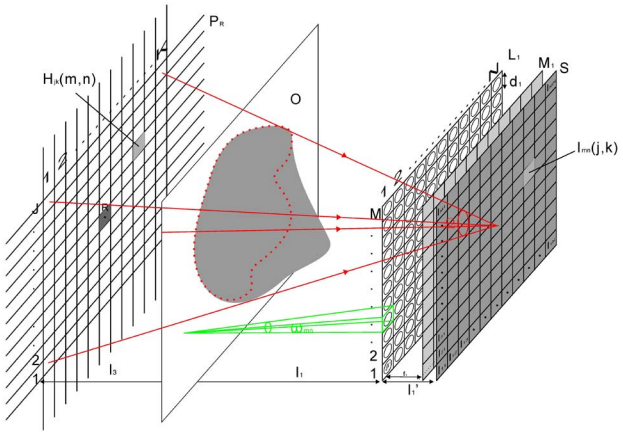

Fig. 1. Sketched map for parallel acquisition of spatial spectrum: $J * K$ hoxels $H_{jk}(m,n)$ are imaged by $M * N$ small lenses to form $M * N$ images $I_{mn}(j,k)$ of the spatial spectrum.

photography, the lens array here is not a microlens array; the aperture a_1 of each lens is big, so as to acquire enough of a distinct image of each spatial spectrum, but it is never bigger than d_1. The focal length f_1 determines the viewing angle $\boldsymbol{\Omega}$ of each individual lens. The bigger the $\boldsymbol{\Omega}$ of the lens, the bigger the scope of the 3D object it can acquire. Here, we suppose that $\boldsymbol{\Omega}$ is big enough to make at least one lens near the center $(M/2, N/2)$ of the lens array acquire the whole object $O(j,k)$, as shown in Fig. 1.

Compared with the work we have described in Refs. [1–5], where the anchoring acquisition was adopted, except for the spatial spectrum image $I_{(M/2)(N/2)}(j,k)$ at the center of the lens array, which is exactly the same, other sub-images are shifted a phase factor of δ_{mn} on the spectrum surface corresponding to the original spatial spectrum $I_{mn}(j,k)$ acquired by the anchoring acquisition. They are then trimmed by the field aperture M_1 to make the reference point R_{mn} on each sub-image of the original object O overlap at the same position R after imaging back to the original space. In Figs. 2 and 3, the corresponding coordinates of the reference point R and its sub-image R_{mn} inside each spatial spectrum are respectively compared. The phase factor δ_{mn} is the inherent character for parallel acquisition described in this Letter; it could be the accordance of each spatial spectrum shift when the 3D data is acquired by the anchoring acquisition and playing back in a parallel situation or vice visa.

2. Holographic coding of the spatial spectrum.

It is necessary here to create holographic coding by making use of the $J*K$ pixels of each $M*N$ spatial spectrum acquired from Fig. 1 to generate the $J*K$ holographic coded spatial spectrum $S_{jk}(m,n)$. The details are shown in Fig. 4. We can use a computer to pick the $(j^{\text{th}}, k^{\text{th}})$ pixel P_{mnjk} of the image $I_{mn}(j,k)$ to fill the inside of a certain hoxel H_{jk} of the object space shown in Fig. 1 to get the coded spatial spectrum $S_{jk}(m,n)$ of this hoxel. The significance of such holographic coding is as follows: (1) We can efficiently realize coordinate transformation between "image and spectrum" to eradicate the fatal drawback of "pseudo-scope imaging." (2) Such a coding

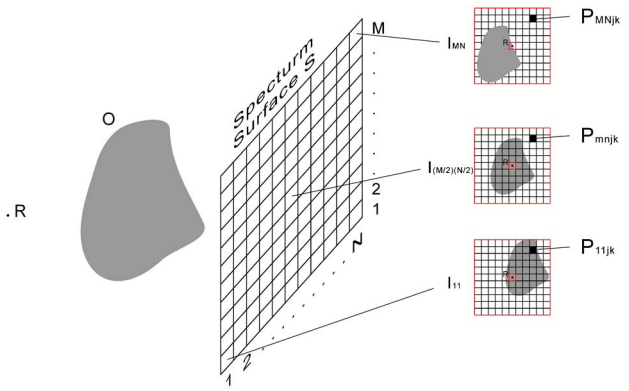

Fig. 2. Sketched map for anchoring acquisition of spatial spectrum in Refs. [1–5]. The reference point R is at the same position inside each individual sub-image.

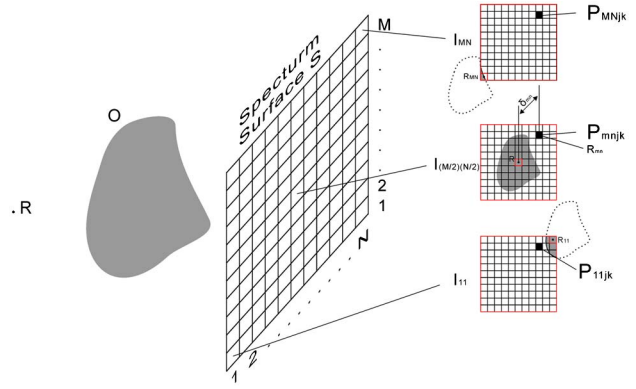

Fig. 3. Sketched map for parallel acquisition of spatial spectrum in this Letter. The sub-image R_{mn} is shifted a phase factor δ_{mn} compared with Fig. 2.

method is versatile and can be used in any kind of 3D display system; the holographic coded image $S_{jk}(m,n)$ can be directly broadcasted by the lens array, or treated as the "hogel" to print the 3D hologram dot by dot[7]. (3) By means of simply magnifying or reducing the pattern size of S_{jk}, the size of the hoxel H_{jk} could be arbitrarily changed to get a magnified or reduced display of a 3D object,. (4) According to the details of acquiring or displaying a 3D space (such as resolution, depth, and viewing angle, etc.), the maximum sampling angle ω_{mn} could be designed for perfect 3D displays by the minimum spatial spectrum number (M,N) for the most efficiency.

3. Recovery of discrete spatial spectrum.

After a simple treatment involving magnifying or reducing, $J*K$ frames of holographic coded image S_{jk} are

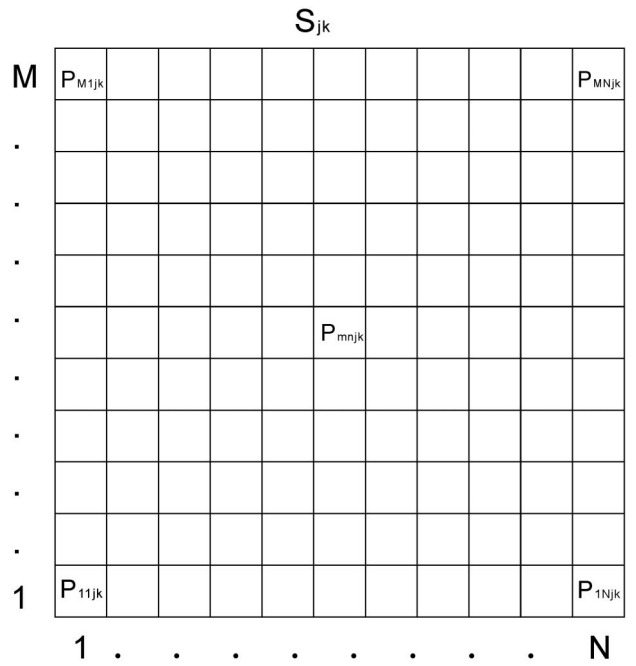

Fig. 4. Sketched map for holographic coded spatial spectrum image S_{jk} of a hoxel H_{jk}.

displayed at the corresponding positions on a flat-panel displayer D, which has a resolution bigger than $M*N*J*K$. Figure 5 is the sketched map for the restoration of the integral discrete spatial spectrum, where lens plate L_2 is located in front of D with a distance of l_2'. l_2 is equivalent to l_3 in Fig. 1 when the hoxels H_{jk} are correspondingly reduced or magnified. L_2 is still comprised by $J*K$ small lenses with the same imaging parameters denoted by a_2 for the aperture of each lens and d_2 for the concentric distance (here is just the hoxel size of the preset H_{jk} in Fig. 1). Field aperture M_2 is also placed between D and L_2 to prevent the crosstalk of each S_{jk}. Each lens on L_2 has the same viewing angle Ω as in the acquisition to avoid the deformation of the final image. As shown in Fig. 5, each coded spatial spectrum $S_{jk}(m,n)$ displayed on the monitor D would be projected backwards as the discrete spatial spectrum $I_{mn}(j,k)$ of the original object used to form a 3D images O' where the number of the preset hoxels H_{jk} is changed from $J*K$ to $J'*K'$ which is number of the final displayed hoxels H'_{jk}. $J'*K'$ is obtained as follows: (1) It is supposed that the pixel size of the displayer D is Δ_D. (2) When S_{jk} is imaged by a lens inside L_2 and the image size is magnified M times, the corresponding hoxel size is $M\Delta_D$. (3) It is supposed that the length and width of the displayer D are respectively a and b. (4) $J'=a/(M\Delta_D)$, and $K'=b/(M\Delta_D)$. It can be seen that $J'*K'$ do not have a direct relation to $J*K$, which is the eventual number of hoxels H'_{jk} that is formed by $M*N$ directional projections from the original hoxel H_{jk}, i.e., the final hoxel resolution of the holographic display inside the display area of $a*b$. Compared with the traditional integral imaging techniques, the lens here is not a microlens; otherwise, the white light speckle noise would be unacceptable. The aperture a_2 of each lens is big, so as to distinguish the features of $S_{jk}(m,n)$, but it is never bigger than d_2.

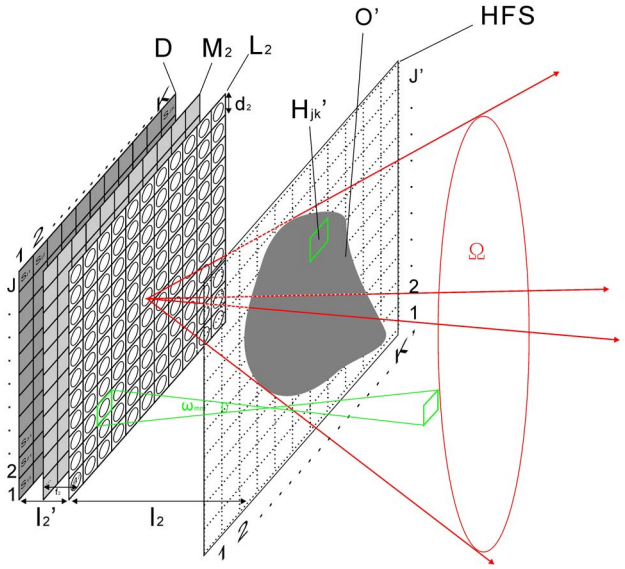

Fig. 5. Sketched map for 3D reconstruction decoded by the HFS.

4. Integral reconstruction decoded by HFS.

As shown in Fig. 5, we placed a corresponding HFS, which is described in our previous work[1–5], at the position of O' to make the expanding angle of each discrete spatial spectrum input S_{jk} the same as the sampling angle ω_{mn} shown in Fig. 1; i.e., to make each coded spatial spectrum S_{jk} combined together but not severely overlapped (the appearance here is a uniform bright background because the edge features of each lens are just smeared together by the HFS). This forms an integrally continuous output of the spatial spectrum. Human eyes can then observe a real holographic 3D image O' floating on the HFS. It should be noted that the HFS should be located at the above-mentioned place; this is the most efficient way to display a certain sampling angle ω_{mn}. The HFS could be regarded as the standard plane straddled by the displayed 3D space with the depth determined by ω_{mn}. When the HFS is not correctly located to make the broadcasting angle much bigger or smaller than the sampling angle, the displayed space would be lack the original 3D data, which would result in severe crosstalk or a nonlinear appearance.

In order to make our innovation more comprehensible, the following analysis was done of the imaging quality:

1. Spatial spectrum description of 3D information:

Suppose Δ_{jk} is the size of a preset hoxel H_{jk} in a 3D space, and ΔZ is the depth of that space, then the corresponding sampling angle can be expressed as $\omega_{mn}=\Delta_{jk}/\Delta Z$. That is to say, a 3D object O constructed by $J*K*\Delta Z*\Delta_{jk}$ individual small cubic irradiators $(\Delta_{jk})^3$ can be completely derived by $M*N*J*K$ individual light tapers, in which the apex of each light taper is located inside the plane of the HFS, while the divergent angle is ω_{mn}. The viewing angle of this 3D object is $\Omega=\Sigma\Sigma\omega_{mn}$.

Here, we have $\Delta Z*\Delta_{jk}=\Delta_{jk}*\Delta_{jk}/\omega_{mn}=M*N$, because $M*N$ spatial spectra are included inside the hoxel H_{jk}.

2. Spatial spectrum description of human vision:

Some basic parameters of human eyes are as follows: (1) pupil distance (the average distance of two eyes) $d_E\approx 6.5$ cm, (2) pupil diameter (2–8 mm, depending on the brightness), on average, is $a_E\approx 5$ mm, (3) angular resolution limitation: $\omega_E\approx 1.5*10^4$, and (4) viewing angle in the stationary state: $\Omega_E\approx 90°$. When human eyes are fixed on a certain position, human vision is able to express $J*K=(\Omega_E/\omega_E)^2\approx[(\pi/2)/1.5*10^4]^2\approx 10^8$ hoxels and needs only two spatial spectra ($M*N=2$) to form the binocular stereoscopic image. There are 10^8 spatial spectra identified by human eyes, included in two hoxels H_R and H_L to form the objective 3D knowledge acquired by human eyes submerged into such hoxel oceans.

3. Effective acquisition and restoration:

Aiming at the spatial spectrum expression described in 1 and 2, the visible 3D space information could be fully acquired by the lens array plate L_1 shown in Fig. 1, and also could be fully restored by the lens array plate L_2 shown in Fig. 5. The detailed requirements are as

follows: $a_1 = 2\lambda l_1/\Delta_{jk}$, $a_2 = 2\lambda l_2/\Delta_{jk}$, λ is approximately 550 nm, which is the average wavelength of visible light, $\omega_{mn} = d_1/l_1 = d_2/l_2$, $\tan(\Omega/2) = a_1/(2f_1) = a_2/(2f_2)$. Here, the sizes of the lens apertures (a_1 and a_2) determine the size of hoxels Δ_{jk} or the cubic voxels $(\Delta_{jk})^3$ that are acquired or restored; the concentric distances (d_1 and d_2) determine the sampling angle ω_{mn} of the space acquired or restored, and therefore determine the depth of this space $\Delta Z = \Delta_{jk}/\omega_{mn}$. The focal lengths ($f_1$ and f_2) determine the viewing angle Ω of this space, which behaves as the processing capability of a lens unit in the spatial spectrum information, i.e., $\Omega = \Sigma\Sigma\omega_{mn}$. Because we adopt the HFS to compromise the nonlinear features of the lens array, the microlens paradox for integral photography could be completely avoided. The key is achieving a high-enough resolution of the corresponding sensor (S in Fig. 1) and displayer (D in Fig. 5) to identify and display the spatial spectrum information composed by above-mentioned $J * K * M * N$ individual pixels.

By making use of a commercially available 4 K flat-panel displayer KKTV LED39K60U with the resolution of $3840 * 2160$, according to the above-mentioned principles, we have achieved a digital holographic display with full color and full parallax. The details of the parameters are as follows: (1) hoxel size is 2.5 mm * 2.5 mm, (2) number of hoxels is $J' * K' = 337 * 188$, (3) the number of the spatial spectrum is $M * N = 36 * 36$, and (4) the viewing angle is $\Omega = 30°$.

Figure 6 is the sketched map of the holographic coded pattern of the spatial spectrum inside each small lens; here, the process of acquisition is replaced by directly rendering the computer-simulated 3D models. In order to fully use the limited pixels on the 4 K displayer, we aligned 3818 small lenses with the aperture $a_2 = 10$ mm diameter in a honeycomb array. Figure 7 is the picture taken from one direction before the HFS is applied. No detailed features can be identified in the picture, only discrete light rays from the hoxel H_{jk}. Figure 8 is the picture taken from one direction after the HFS is applied. All features are properly decoded by the HFS as the final displayed hoxel H'_{jk}. Figure 9 shows the pictures taken from multiple directions of the holographic displayed digital 3D models formed by the coded spatial spectrum shown in Fig. 6; the smooth color restoration and the full parallax relationship of the displayed space can be distinctly seen. Figure 10 is another result of a holographic display "skull" in which each profile is clearly expressed.

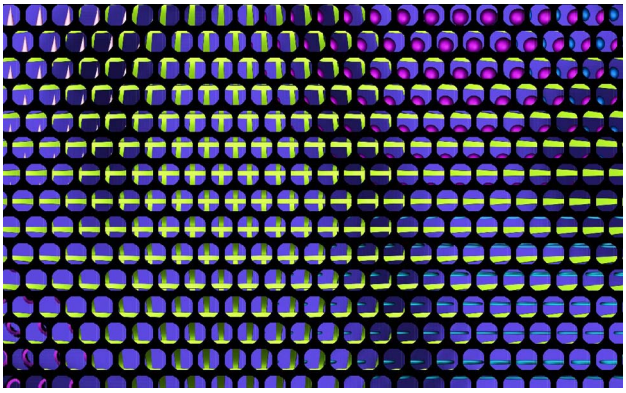

Fig. 6. Sketched map of holographic coded pattern of the spatial spectrum inside each small lens.

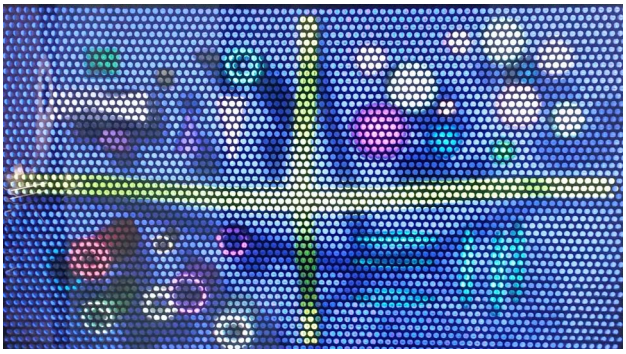

Fig. 7. Sketched map for restoration before the HFS is applied.

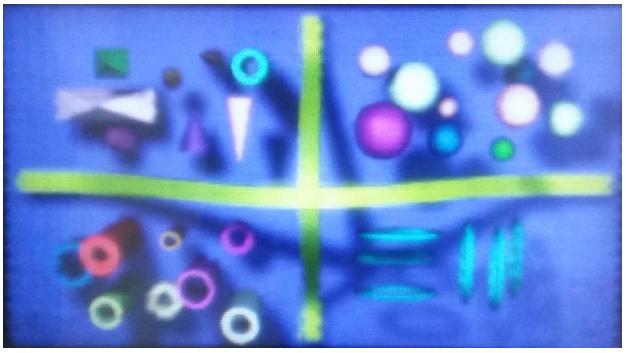

Fig. 8. Sketched map for restoration after the HFS is applied.

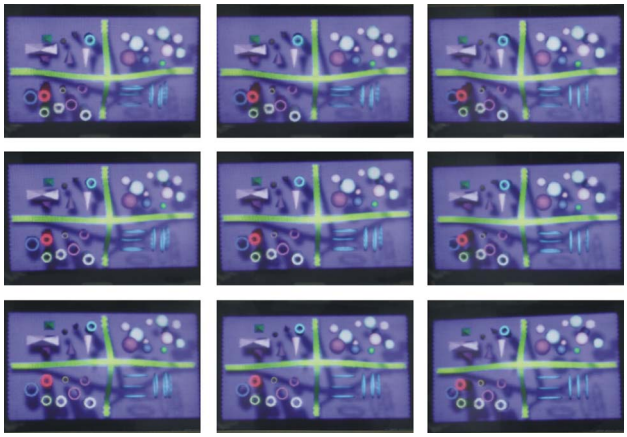

Fig. 9. Pictures taken from multiple directions of the holographic display digital 3D models. Q1: Can you find out any differences between the 9 pictures? Q2: Can you imagine the 3D relations of each object only with the clues of such differences? It would be eye seeing in site for real 3D display.

Fig. 10. Pictures taken from multiple directions of the holographic display digital 3D "skull."

In conclusion, we demonstrate the design and experimental result of identifiable holographic display for human vision. The key is to transform the visual redundant pixels into an identifiable hoxel display. Although the available 4 K flat-panel displayer could only obtain a 2.5 mm hoxel size, the developing 8 K or even 16 K flat-panel displayer would eventually improve the final hoxel resolution for the eye-catching level if the lens aperture is bigger than the human pupil. We expect this novel device would find its first application in medical imaging, with the obvious advantage of seeing $36 * 36$ pictures in real 3D form simultaneously.

We acknowledge the standing support of all staff members from AFC Technology Co., Ltd. for their hard work to obtain financial support for this breakthrough.

References

1. F. C. Fan, S. Choi, and C. C. Jiang, in *Proceedings of the Eighth International Symposium on Display Holography* 424 (2009).
2. X. Shang, F. C. Fan, C. C. Jiang, S. Choi, W. Dou, C. Yu, and D. Xu, Opt. Lett. **34**, 3803 (2009).
3. F. C. Fan, S. Choi, and C. C. Jiang, Appl. Opt. **49**, 2676 (2010).
4. C. Yu, J. Yuan, F. C. Fan, C. C. Jiang, S. Choi, X. Sang, C. Lin, and D. Xu, Opt. Express **18**, 27820 (2010).
5. F. C. Fan, S. Choi, and C. C. Jiang, in *Techniques and Principles in Three-Dimensional Imaging: An Introductory Approach* (IGI Global, 2014), Chap. 8.
6. H. I. Bjelkhagen, in *Techniques and Principles in Three-Dimensional Imaging: An Introductory Approach* (IGI Global, 2014), Chap. 6.
7. M. A. Klug, A. Klein, W. J. Plesniak, A. B. Kropp, and B. Chen, Proc. SPIE **3011**, 78 (1997).